Experiments in Fluids 19 (1995) 405–416 © Springer-Verlag 1995

Direct drag measurements in a turbulent flat-plate boundary layer with turbulence manipulators

T. B. Lynn, D. W. Bechert, D. A. Gerich

Abstract The effect of turbulence manipulators on the turbulent boundary layer above a flat plate has been investigated. These turbulence manipulators are often referred to as Large Eddy Break Up (LEBU) devices. The basic idea is that thin blades or airfoils are inserted into the turbulent flow in order to reduce the fluctuating vertical velocity component v' above the flat plate. In this way, the turbulent momentum transfer and with it the wall shear stress downstream of the manipulator should be decreased. In our experiments, for comparison, a merely drag-producing wire also was inserted into the boundary layer.

In particular, the trade-off between the drag of the turbulence manipulator and the drag reduction due to the shear-stress reduction on the flat plate downstream of the manipulator has been considered. The measurements were carried out with very accurate force balances for both the manipulator drag and the shear stress on the flat plate. As it turns out, *no net drag reduction is found* for a fairly large set of configurations. A single thin blade as a manipulator performed best, i.e., it was closest to break-even. However, a further improvement is unlikely, because the device drag of the thin blade elements used here has already been reduced to only that due to laminar skin friction, and is thus the minimum possible drag. Airfoils performed slightly worse, because their device drag was higher. A purely drag-producing wire device performed disastrously. The wire device, which consisted of a wire with another thin wire wound around it to suppress coherent vortex shedding and vibration, was designed to have (and did have) the same drag as the airfoil manipulator with which it was compared. The comparison showed that airfoil and blade manipulators recovered 75–90% of their device drag through a shear-stress reduction downstream, whereas the wire device recovered only about 25–30% of its device drag.

Conventional LEBU manipulators with airfoils or thin blades produce between 0.25% and 1% net drag increase, whereas the wire device (with equal device drag) produces as much as 4% net drag increase. These data are valid for the specific plate length of our experiments, which was long enough in downstream extent to realize the full effect of the LEBU manipulators. Turbulence manipulators do indeed decrease the turbulent momentum exchange in the boundary layer by "rectifying" the turbulent fluctuations. This generates a significant shear-stress reduction downstream, which is much more than just the effect of the wake of the manipulator. However, the device drag of the manipulator cannot be reduced without simultaneously reducing the skin friction reduction. Thus, the manipulator's device drag exceeds, or at best cancels, the drag reduction achieved by the shear-stress reduction downstream. A critical survey of previous investigations shows that the suggestion that turbulence manipulators may produce net drag reduction is also not supported by the available previous drag force measurements. The issue had been stirred up by less conclusive measurements based on local velocity data, i.e., data collected using the so-called momentum balance technique.

List of symbols

b	lateral breadth of test plate
c	chord length of turbulence manipulator
d	diameter of wire manipulator
e	distance of the elastic center from the leading edge of the manipulator airfoil
h	height of manipulator above test plate
q	dynamic pressure of the potential flow above the test plate
s	spacing of turbulence manipulator elements
t	thickness of turbulence manipulator elements
u',v',w'	fluctuating velocities in downstream, plate-normal, and lateral directions
x	distance from the leading edge of the test plate in the downstream direction
x_o	location of the trailing edge of the first manipulator
z	distance from test plate center in the lateral direction
C_D	drag coefficient
C_L	lift coefficient

Received: 27 March 1995/Accepted: 17 July 1995

T. B. Lynn
DEXSIL Corporation, 1 Hamden Park Drive,
Hamden, Connecticut 06517, USA

D. W. Bechert
DLR, Abt. Turbulenzforschung, Müller-Breslau-Str. 8,
D-10623 Berlin, Germany

D. A. Gerich
Hochschule Wismar, Fachbereich Maschinenbau-Strömungslehre,
Philip-Müller-Str. 1, D-23952 Wismar, Germany

Correspondence to: D. W. Bechert

The authors would like to thank Prof. H. H. Fernholz for his scientific and administrative support. The hardware for the experiments was designed and built by C. Daase, W. Hage and R. Makris. Funding for the project was provided by the Deutsche Forschungsgemeinschaft and is gratefully acknowledged.

D_m drag of manipulated plate including device drag and shear stress, calculated from manipulator location to downstream location ξ

D_o drag of unmanipulated plate boundary layer, consisting of the shear stress calculated from manipulator location to downstream location ξ

F drag force

F_o total skin friction force, measured over a distance from 0.4 m upstream of manipulator to 6.35 m downstream of manipulator, measured without turbulence manipulator

F_{LEBU} device drag force of the LEBU, i.e., the turbulence manipulator

F_m total drag force of manipulated plate, consisting of F_{LEBU} and skin friction force, measured over a distance from 0.4 m upstream of manipulator to 6.35 m downstream

F_{cf} skin friction force as measured by the floating element balance, manipulated case

F_{cfo} skin friction force, as measured by the floating element balance, unmanipulated case

ΔF_{cf} skin friction saving, defined as $\Delta F_{cf} = F_{cf} - F_{cfo}$

$\sum F_{cf}$ cumulative skin friction savings, i.e., the sum of the skin friction savings ΔF_{cf}, added up from the location of the manipulator to the downstream location ξ, as shown in Fig. 11. In Fig. 13 the cumulative skin friction savings are summarized up to their asymptotic value, reached at $\xi \approx 200$

Re_c Reynolds number of the manipulator elements, calculated with the chord length c and the local velocity in the boundary layer

Re_θ Reynolds number at the location x_o of the manipulator, calculated with the momentum thickness θ of the boundary layer and the mean flow velocity U_∞

U_∞ mean flow velocity in the potential regime of the wind tunnel test section

α angle of attack of the manipulator airfoils

δ_o boundary layer thickness at the location x_o of the manipulator

ξ dimensionless distance from the manipulator in the downstream direction, defined as $\xi = (x - x_o)/\delta_o$

ρ density of the air

τ_o local skin friction shear stress, unmanipulated case

$\tau_{o_{\mathrm{Average}}}$ skin friction shear stress, average value over the lateral span ($b = 2$ m) of the test plate, unmanipulated case

τ_m local skin friction shear stress, manipulated case

θ momentum thickness of the undisturbed turbulent boundary layer at the location x_o

1 Introduction

The suggested possibility of large net drag savings has drawn many researchers into the field of turbulent boundary layer manipulation. The most common outer layer manipulation device consists of one or more thin flat ribbons or airfoils immersed in the boundary layer. The devices are suspended above the primary flat plate at a height between $0.4\,\delta_o$ and $0.9\,\delta_o$, where δ_o is the unmanipulated boundary layer thickness. The devices generally have a chord length on the order of δ_o and a thickness between $0.1\,\delta_o$, for airfoils, and 0.005–$0.01\,\delta_o$, for ribbon-type devices, see Fig. 1.

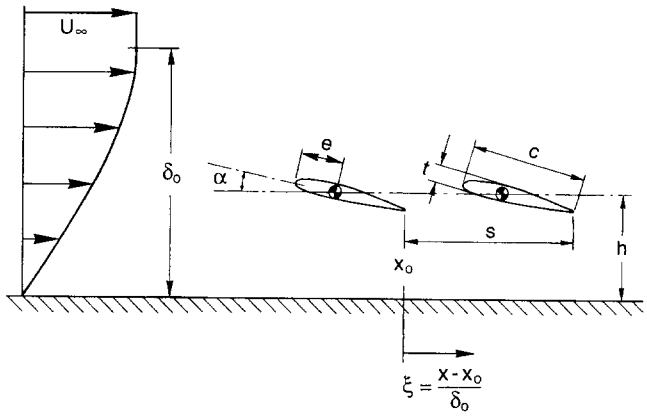

Fig. 1. Schematic of LEBU device showing relevant parameters, α = angle of attack, c = chord length, t = thickness of the LEBU, h = height above the plate and s = spacing. The location of the elastic center of the LEBU is $e = 0.42c$ from the leading edge for the airfoil and $e = 0.5c$ for the ribbon LEBU. x_o is the location of the trailing edge of the first LEBU; δ_o is the thickness of the boundary layer at x_o

There exists a large body of reliable data documenting the effects of LEBU manipulators on the structure of a turbulent boundary layer. Some of the most commonly reported effects on boundary layer structure are presented in Table 1. The majority of these effects have been measured using either single or multiple hotwires, crossed wires or a combination of them. Over the range of possible LEBU configurations these alterations are generally self consistent in that they can be reproduced easily by different laboratories and they follow logically changes in LEBU geometry.

The interpretation of these effects on the boundary layer has in most cases been made with the *a priori assumption* that a net drag reduction was a *real* phenomenon. The determination of a net drag change hinges critically on the accurate measurement of total drag on two different systems: on a simple fully developed flat plate boundary layer and, on the other hand, on an altered boundary layer containing a manipulation device having an inherent drag of its own. The most commonly used method of determining total drag is the so-called "momentum balance" requiring the measurement of velocity profiles along the streamwise axis. The determination of the total drag on two different systems using momentum balance techniques (which can be made to work on standard normal boundary layers reasonably well) is not a straightforward proposition, resulting in fairly large systematic errors in net drag determination. A brief critical discussion of this issue can be found in Bandyopadyay's (1986) review article. These systematic errors have led to widely varying drag reduction results obtained for nominally similar LEBU configurations. Figure 2, which shows the local skin friction distributions obtained by different research groups using relatively simple "ribbon" type LEBUs in nominally similar configurations, indicates the degree of scatter in the published data.

One proposed explanation for the large scatter in the published data has been the low chord Reynolds numbers characteristic of these devices. It is well known that low chord

Table 1. Observed LEBU effects on the boundary layer

	Bertelrud et al. 1982	Blackwelder & Chang 1986	Bonnet et al. 1987	Corke 1981	Corke et al. 1979	Coustols & Cousteix 1985	Guezennec & Nagib 1990	Hefner et al. 1981	Lemay et al. 1985	Lemay et al. 1989	Lynn 1987, 1989	Mangus 1984	Mumford & Savill 1984	Nagib et al. 1984	Nguyen et al. 1984	Nguyen et al. 1987	Savill 1987	Veuve et al. 1989	Westphal 1986
Altered u' and v' Profiles		X	X			X	X			X							X	X	X
Altered Mean Flow Angles							X												
Altered Turbulent Production Profiles							X												
Altered Reynolds Stress Profiles			X			X	X			X							X	X	X
Altered Intermittency Profiles							X												
Altered Length Scales		X									X								
Law of Wall Not Altered									X		X				X	X	X	X	X
Altered Taylor Microscale (but Recovers by $27\delta_0$)		X																	
Altered Cross Correlations		X									X								
Altered Flow Visualization "Structures"				X									X						
Altered Iso-Correlations		X								X	X								
Altered Time Scales							X							X					
Altered Pressure Distribution Under Device																	X		
Altered w' Profiles			X							X									
Altered u Velocity Spectra			X							X									
Altered Turbulent Kinetic Energy			X																
Bursting Frequency (VITA) (Change Difficult to See)												X							
Altered u' Profile	X				X			X			X								
Altered Log Law (Only when C_f Indirectly Measured)	X				X							X							

Reynolds number airfoils are very sensitive to small spanwise variations affecting laminar separation, resulting in a somewhat sporadic behavior (reflected in the drag coefficient C_D; Anders 1986). An examination of the available data on the effects of chord Reynolds number on the performance of all types of LEBUs, including airfoil-shaped devices, was undertaken. The results are shown in Fig. 3, where the degree of drag reduction found is plotted against chord Reynolds

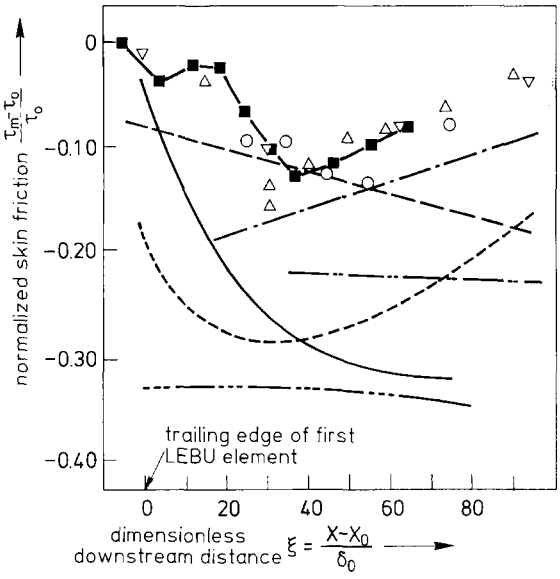

Fig. 2. Local skin friction distribution downstream of ribbon-type tandem LEBU's obtained by both direct and indirect methods. Wall shear stresses: τ_o = unmanipulated, τ_m = manipulated. LEBU parameters: $\alpha = 0°$; $h/\delta_o \approx 0.75$; $Re_c \approx 30{,}000$; $c/\delta_o \approx 1$; $7 < s/\delta_o < 12$ (Symbols: Oil-film interferometry: ○ Westphal (1986); Drag force balance: △ Lemay et al. (1985), ▽ present data; Sublayer fence: ■ Lynn (1987); Momentum balance: -·-· Corke (1981), -···- Corke et al. (1982), —— Bertelrud et al. (1982), — — — Hefner et al. (1983), ---- Plesniak (1984); -·- Anders and Watson (1985))

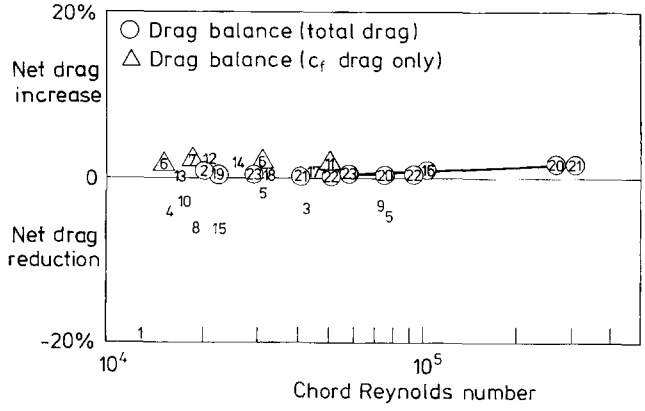

Fig. 3. Net drag performance of LEBU manipulators versus chord Reynolds number for all types of LEBU's.
1 Corke (1981); *2* Hefner et al. (1981); *3* Bertelrud et al. (1982); *4* Hefner et al. (1983); *5* Anders et al. (1984); *6* Mumford and Savill (1984); *7* Nguyen et al. (1984); *8* Plesniak (1984); *9* Anders and Watson (1985); *10* Coustols and Cousteix (1985); *11* Lemay et al. (1985); *12* Poddar and van Atta (1985); *13* Bandyopadhyay (1985); *14* Papathanasiou and Nagel (1986); *15* Rashidnia and Falco (1986); *16* Sahlin et al. (1986); *17* Westphal (1986); *18* Lynn (1987); *19* Poll and Westland (1987); *20* Sahlin et al. (1988); *21* Anders (1989); *22* Lynn et al. (1989); *23* Present data

number of each device. As Fig. 3 shows, there is indeed a large scatter at low Reynolds numbers, but only among the data acquired with the indirect momentum balance.

A much stronger correlation is obtained, however, when the method of measuring net drag reduction is considered. Although both net increases and decreases have been found in experiments using indirect methods of measurement (e.g., momentum balance), the experiments using direct methods (i.e., drag balances), indicated by circles in Fig. 3, have not found a net drag reduction at any chord Reynolds number.[1] Direct LEBU performance measurements in other configurations than a flat plate boundary layer show no explicit hints on loss reductions either; see, e.g., the experiments by Prabhu et al. (1987) carried out in a narrow two-dimensional channel and the data by Pollard et al. (1989), collected in a circular tube. Notice also that as shown in Fig. 2, the variation within the momentum balance data is considerably larger than the variation within the results obtained with other techniques to measure turbulent shear stress, although the differences in LEBU geometry are equivalent between the two groups.

The large range of drag reductions reported in the literature has led to the general overestimation of the magnitude of the effect to be expected from LEBU manipulators. For example, the device drag of a tandem NACA 0009 LEBU is typically 5% of the total skin friction drag on the test plate. In their optimum configuration these devices produce a net increase in total drag of only 1%. It is this range of a few percent that reflects the effect of LEBU manipulators in a turbulent boundary layer, and it is with this proper view to the magnitude of the effect that is expected that experiments need to be designed. The uncertainty of momentum balance techniques for normal boundary layers is typically quoted as $\pm 5\%$. Therefore, many of the conclusions about "optimum configuration" and mechanisms of drag reduction based on indirect methods need to be reexamined using accurate direct drag measurements.

Unfortunately, the body of direct drag measurements is relatively small and limited mostly to water towing tank measurements at higher chord Reynolds numbers. In particular, accurate measurements at lower and medium Reynolds numbers are lacking,[2] in a regime where the most spectacular net drag reductions had been claimed previously. With this in mind, we have undertaken to make direct drag measurements using both NACA 0009 airfoil LEBUs and ribbon-type LEBUs at chord Reynolds numbers from 30,000 to 100,000. For our measurements, the momentum thickness Reynolds number of the boundary layer at the location of the first LEBU was between $Re_\theta = 3{,}000$ and 8,850. These experimental conditions are comparable to previous ones. However, our experiments are different in as far as we have carried out both device drag *and* shear stress distribution measurements simultaneously and by direct force measurements.

[1] Although the data published in Anders (1989) indicate that at the lowest Reynolds number tested a small reduction is possible (approximately 3%), the author pointed out that due to the large wave drag in the towing tank at these speeds, the error bars were much larger than the drag reduction.

[2] Except Poll and Westland's (1987) data which were, at that time, at variance with most other published results.

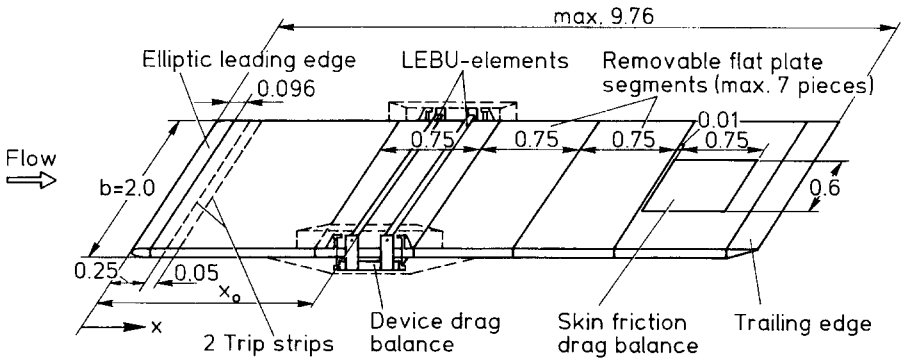

Fig. 4. Schematic of plate with device drag balance and floating wall element skin friction balance. Dimensions in meters. $x_o = 2.95$ m for the "high speed" case and $x_o = 1.73$ m for the "low speed" case

The error bars for the direct drag measurements made here are estimated to be ca. $\pm 0.5\%$.

Finally, it should be noted that the percentage drag reduction (or increase) depends directly on the drag force used to normalize the data (i.e., the drag on the flat plate), and is thus directly dependent on the length of the test plate. We have chosen a plate length long enough to allow the wall shear stress in the manipulated boundary layer to return to unmanipulated values. This means, in real terms, that the maximum effect has been extracted from the manipulators. For longer plates, the percentage drag reduction or increase (i.e., measured drag change normalized with the unmanipulated flat plate drag) would indeed be smaller, the sign of the change will not be affected, and the absolute value of the force savings remains constant. When comparing drag reduction data, it is important to keep this fact in mind, and comparisons among data from different test plates must account for plate length differences.

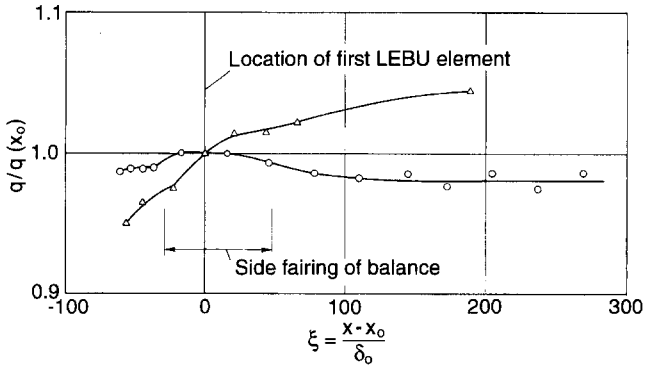

Fig. 5. Dynamic pressure $q = \rho U^2/2$ in the potential flow above the plate, normalized with q taken at the reference position x_o (where the device is located for the manipulated case). Symbols: $\triangle$ = "high speed" experiments with wind tunnel walls parallel to the plate. The mean flow is slightly accelerated due to the displacement effect of the boundary layers. $\bigcirc$ = "low speed" experiments with almost zero pressure gradient, produced by a non-parallel upper wall of the wind tunnel

2
Experimental set-up

The experiments presented here were conducted in two groups: a "high speed" set using either NACA 0009 profiled LEBUs or a WIRE device and a "low speed" set using ribbon type LEBUs. The "high speed" tests were run at free stream velocities of 22.4 and 37.9 m/s, the latter being the highest possible velocity in our low speed wind tunnel. The LEBU-airfoil in these tests, NACA 0009, has been used in previous high Reynolds number towing tank experiments (Sahlin et al. 1986, 1988; Anders 1989). Our wind tunnel has a test section 2 m × 1.4 m and 10 m long. The test plate (see Fig. 4) is suspended horizontally along the center line of the wind tunnel. As the closed test section has constant rectangular cross-section in the streamwise direction, a weak favorable pressure gradient is generated on the test plate, see Fig. 5.

A second "low speed" (15.6 m/s) test series was then carried out in order to match the flow conditions of the earlier experiments in which conspicuously high net drag reductions had been reported (references see Fig. 3). In order to make our data as conclusive as possible we thought it preferable to have zero pressure gradient on the test plate. Therefore, the wind tunnel test section was fitted with a slightly divergent upper wall to achieve this (see Fig. 5).

The aluminium flat plate test surface (see Fig. 4) could be varied in length from 2.55 to 9.76 m by adding or removing segments. Each segment was constructed as a 5 cm thick hollow "sandwich", with a 6.35 mm thick ground ALCOA aluminium plate as the top surface and a 3 mm aluminium sheet forming the bottom layer. After segments were added or removed, the segment joints were carefully adjusted to ensure that no steps or gaps existed larger than 0.05 mm. The leading edge of the test plate has a cross section of a half-ellipse with a 1 : 4 axis ratio. The two turbulator strips are DYMO plastic adhesive tapes 12.6 mm wide and 0.4 mm thick, with embossed V-letters pointing in the upstream direction. The embossed V's protrude 0.5 mm above the plastic strip and have a letter size of 5 mm. The flat plate is equipped with two accurate independent drag balances, one measuring the skin friction drag and the other measuring the device drag. The skin friction drag balance is a floating wall element type measuring 75 cm in the streamwise direction and 60 cm spanwise. (For a complete description, see Bechert et al. 1985). By this arrangement, the measurements are confined to the inner region of the test plate where no distortion of the boundary layer by side wall effects can occur. The device drag balance consists of a steel frame suspended on spring steel rods. The LEBU tensioning devices, specially designed to allow adjustment of height, angle of attack, and separation, are attached to the steel frame. The displacement of the frame due to drag on the manipulators is registered by twin differential inductive displacement transducers (Hottinger–Baldwin Q11) with a maximum

displacement of 0.2 mm. The entire balance is located below the flat plate, with only the arms of the tensioning devices protruding above the plate. Streamlined fairings enclose the entire balance both above and below the plate so that only the LEBU device is subject to drag forces.

The flat plate segments each have a streamwise extent matching that of the skin friction drag balance. The device drag balance is affixed to one such segment, and therefore, by adding additional segments between the device drag balance and the skin friction balance, the complete integrated skin friction drag along the streamwise axis can be measured while simultaneously measuring the device drag directly (see Fig. 4).

The symmetric NACA 0009 LEBU elements with a chord length c of 40 mm and thickness t of 3.6 mm were milled out of solid tempered aluminum using a specially manufactured milling tool. A more practical technique for producing aluminum NACA 0009 profiles in 2 m lengths by cold extrusion was also used. The drag characteristics of the two types of NACA 0009 profiles were compared; there was very little difference, although the extruded LEBUs had a somewhat blunter trailing edge. Since one hypothesized mechanism for LEBU interaction, namely the interaction of the vorticity shed from the device railing edge due to instantaneous changes in C_L as turbulent eddies pass (vortex unwinding), requires a sharp trailing edge, all subsequent high speed net drag measurements were made using the milled NACA 0009 profiles.

The LEBU devices used for the low speed experiments were of the thin ribbon type, constructed of either 0.15 mm × 60 mm or 0.20 mm × 30 mm polished spring steel stock. (The thicker bands were used for the 30 mm LEBUs to eliminate flutter problems.) Each LEBU was carefully prepared by clamping the spring steel stock between two steel plates and hand-grinding the edge, using first a coarse sharpening stone followed by a fine stone, and finishing with fine polishing paper. This process was repeated on each edge at two angles, 45° and 20°, resulting in a compound angle with no sharp corners. The number of passes with each stone at each angle was varied to obtain either a rounded or a tapered edge (see Fig. 7, inset). The resulting edges were then inspected under a microscope to ensure that they had the proper shape and were uniform over the entire span.

The WIRE device used in the "high speed" experiments consisted of two 0.5 mm diameter spring steel wires, each wrapped by a 0.2 mm spring steel wire to help prevent vortex shedding from exciting resonances in the wire. The Reynolds number Re_c is here calculated with the diameter of the center (0.5 mm) wire.[3] The wire diameter combination was chosen so that the device drag of the WIRE device would match that of the LEBU device. A comparison of the skin friction reductions produced by the LEBU and WIRE devices provides information on the relative contributions due to the wake effects and the chord length effects.

Strain gauges fitted to each end holder of the LEBU's were used to ensure that the devices were not vibrating during a test run. The output from the strain gauge bridge was frequency analyzed to ensure there were no strong discrete peaks, which would have indicated flutter. The strain gauges were also used to determine the tensioning force. For each ribbon type LEBU set-up, the LEBU tension was adjusted so that the first string resonance mode was 50 Hz ($T = 300$ N/mm^2), see Morse and Ingard (1968). The profiled LEBUs required only a tension of 70 N/mm^2 to eliminate flutter.

For each plate configuration, the skin friction balance, the device drag balance, and the LEBU strain gauges were recalibrated using weights. The skin friction drag and the device drag were then measured for each of the LEBU configurations as well as for the unmanipulated case. The apparent device drag registered with no device mounted was used as a correction for aero-elastic flexing of the device drag segment as well as a check for errors caused by small leaks in the fairing. Additionally, the skin friction drag was measured both before and after the manipulated cases, in order to obtain statistics on the reproducibility of the skin friction measurements and the overall total accuracy of the drag reduction estimates. To minimize thermal effects due to heating of the wind tunnel, the experiments were run in a timed sequence: ramping the wind tunnel speed from zero to the desired speed, allowing the drag balances to reach a stable value, noting the balance readings and the flow conditions, and then ramping back to zero. This allowed for zero-drift correction, resulting in an average standard deviation for both force measurements of approximately 0.1% of the measured force. For the "high speed" experiments each data point was an average over four cycles. In the "low speed" experiments three cycles were averaged, because the data scatter was lower there, due to a smaller temperature drift of the wind tunnel.

The combined data from the "high speed" and "low speed" experiments are presented in Tables 2a, b and c. Three types of manipulators were investigated: NACA 0009 profiles, WIRE manipulators and ribbon-type LEBUs. The manipulator parameters were chosen after the published data were analyzed to determine the characteristics of LEBU devices for which net drag reductions have been reported, and thus those most likely to result in a net drag reduction when measured directly. The WIRE manipulator was then chosen to have the same device drag as the NACA 0009 LEBU device and was configured identically. This provided an excellent control experiment to isolate the wake effects of manipulators from other possible mechanisms.

The data in the last two rows of Tables 2a, b and c were collected as follows: The drag force on the manipulators is F_{LEBU}. This drag force is measured on LEBU's of ca. 2 m length and is normalized to the lateral extent of the shear force balance, i.e., 0.6 m. The shear force on the unmanipulated test plate is F_o. It consists of the sum of 9 τ-measurements under and downstream of the manipulator location (x_o), collected with the floating element skin friction balance (see Fig. 4). The leading edge of this τ-sensitive regime starts at 0.4 m upstream of the location of the first manipulator x_o and it extends over a total length of 6.75 m ($= 9 \times 0.75$ m) in the downstream direction. This configuration of the skin friction measurements is valid for all of our data. The ratio F_{LEBU}/F_o highlights the relative magnitude of the effect that can be expected from devices such as these. In the last row, F_m represents the sum of

[3] We admit that this definition of Reynolds numbers (albeit common) is counterintuitive, because quite different numbers occur for bodies experiencing identical mean flow and drag conditions.

Table 2a. LEBU Parameters Investigated – NACA 0009 Airfoil ("high speed" experiments)

Type	NACA 0009							
Config.	TANDEM							
U_∞	22.4 m/s				37.9 m/s			
Re_θ	5,760				8,850			
s/δ_o	7.78				8.00			
c/δ_o	1.15				1.18			
h/δ_o	0.49	0.77			0.50	0.80		
Re_c	52,000	57,000			88,000	96,000		
t/δ_o	0.104	0.104			0.107	0.107		
α	0	$-2°$	0	$+2°$	0	$-2°$	0	$+2°$
F_{LEBU}/F_o	0.0521	0.0656	0.0576	0.0582	0.0469	0.0608	0.0511	0.0537
F_m/F_o	1.0135	1.0266	1.0212	1.0243	1.0100	1.0275	1.0170	1.0234

Table 2b. LEBU Parameters Investigated – WIRE Device ("high speed" experiments)

Type	WIRE			
Config.	TANDEM			
U_∞	22.4 m/s		37.9 m/s	
Re_θ	5,760		8,850	
s/δ_o	7.78		8.00	
c/δ_o	0.0144		0.0148	
h/δ_o	0.49	0.77	0.50	0.80
Re_c	650	713	1,100	1,200
t/δ_o	0.0144	0.0144	0.0148	0.0148
α	—	—	—	—
F_{LEBU}/F_o	0.0478	0.0551	0.0515	0.0594
F_m/F_o	1.0367	1.0390	1.0388	1.0409

the 9 shear stress measurements *with* the manipulator in place *plus* the manipulator drag force (F_{LEBU}). Thus the ratio F_m/F_o represents the total drag of the manipulated LEBU + plate system divided by the drag of the unmanipulated plate. We see an effect of the order of a few percent, as expected. The implications of these data will be discussed in the results section.

3 Results and discussion

Prior to conducting the net drag experiments, it was first necessary to investigate the flow over the flat plate without manipulators. An important aspect of this qualification was the verification that the stepwise extension of the flat plate is a reasonable equivalent to moving the skin friction balance along the streamwise axis of a flat plate of fixed length. (In order to achieve the required accuracy, the skin friction drag balance had to be stably mounted in one location and could not be moved). The development of the boundary layer over the flat plate was investigated by measuring velocity profiles along the centerline of a flat plate configuration of various lengths, as well as directly over the skin friction drag balance for plates of successively longer lengths. It was found from the boundary layer and momentum thicknesses that the boundary layer growth is a function only of the distance from the leading edge, not of the specific plate configuration.

To address the issue of two-dimensionality of the boundary layer, the local skin friction was measured across the flat plate in the low speed configuration with a Preston tube at various streamwise distances, see Fig. 6. The data cover the inner part of the flat plate where the floating element balance is located. The lateral dimension z is normalized with the test plate breadth $b = 2$ m (see Fig. 4). The variations across the flat plate were on the order of 5%. There was a systematic elevation of skin friction along the centerline, indicating that there was most likely some very weak secondary flow in the wind tunnel test section.[4] This three-dimensionality of the boundary layer would have an effect on net drag measurements made using local skin friction determinations and in fact points to one of the drawbacks to local measurements. The net drag determinations made here use a skin friction drag balance 1/3 the span in extent and therefore are relatively insensitive to

[4] As a matter of fact, local shear stress variations of much higher magnitude are common and have been reported previously also for nominally constant mean flow distributions (see Head and Rechenberg 1962). Thus, these variations should not be confused with the properties of our mean flow, which has a very even distribution. A fairly detailed series of measurements on mean flow properties, boundary layer and shear stress distribution has been performed by Bruns, et al. (1992) for the present facility.

Table 2c. LEBU Parameters Investigated – Ribbon Type Device ("low speed" experiments)

Type	RIBBON					
Config.	TANDEM		SINGLE			
U_∞	15.6 m/s		15.6 m/s			
Re_θ	2,930		2,930			
s/δ_o	11.5		—			
c/δ_o	1.276		1.276		2.552	
h/δ_o	0.5	0.75	0.5	0.75	0.5	0.75
Re_c	27,000	30,000	27,000	30,000	54,000	60,000
t/δ_o	0.0085	0.0085	0.0085	0.0085	0.0064	0.0064
α	0	0	0	0	0	0
F_{LEBU}/F_o	0.0420	0.0470	0.0220	0.0246	0.0318	0.0339
F_m/F_o	1.0062	1.0143	1.0024	1.0087	1.0062	1.0125

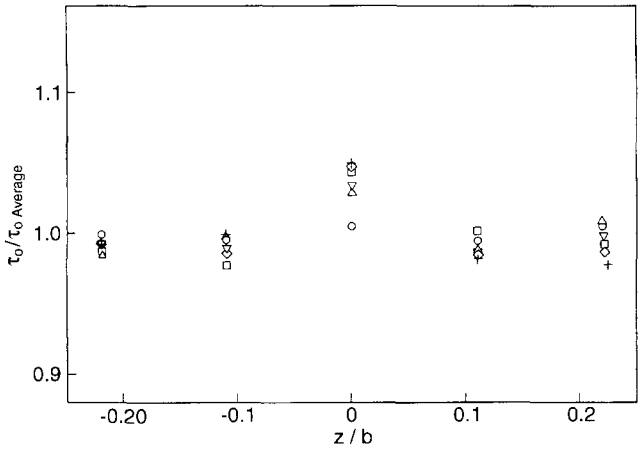

Fig. 6. Spanwise variation of local skin friction measured at various streamwise locations, using a Preston tube of 1.2 mm diameter, unmanipulated boundary layer. Symbols for the streamwise location x: ○ ≙ 0.645 m, △ ≙ 1.395 m, ▽ ≙ 2.145 m, □ ≙ 2.895 m, ◇ ≙ 3.645 m, + ≙ 4.395 m. The data cover the lateral extent (60 cm) of the floating element shear stress balance

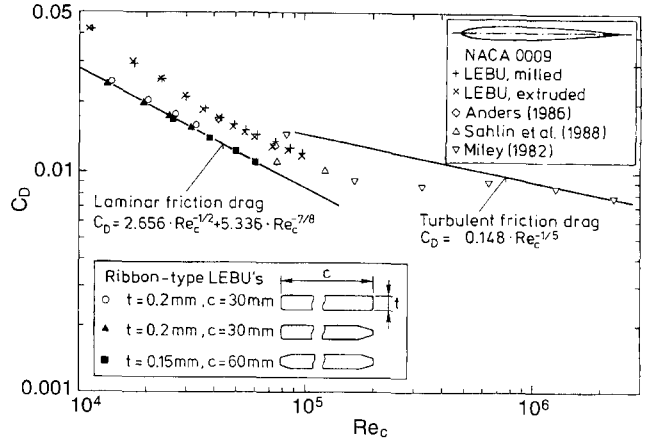

Fig. 7. Drag coefficients for ribbon-type and airfoil LEBUs in freestream flow as a function of chord Reynolds number. The curves for laminar and turbulent skin friction drag are given according to Schlichting (1982)

spanwise distribution of skin friction. Furthermore, since a direct comparison is made between manipulated and unmanipulated drag, the exact nature of the boundary layer is of interest only in determining that its development is normal.

After the boundary layer was determined to be satisfactory, the prepared LEBUs were tested in the freestream flow above the boundary layer. All of the NACA 0009 profiled LEBUs had a C_D approximately 30% above that expected from laminar skin friction drag. This was identical to previously published data on thin airfoil LEBUs (Anders 1986), see Fig. 7. The ribbon-type LEBUs with various edge shapes were also tested in the freestream above the flat plate. It was found that the tapered trailing edge LEBUs had a slightly lower C_D than the LEBUs with rounded edges (see Fig. 7). Although the difference amounted to only 2%, all "low speed" experiments reported here were run using the tapered trailing edge LEBUs. The drag data for the

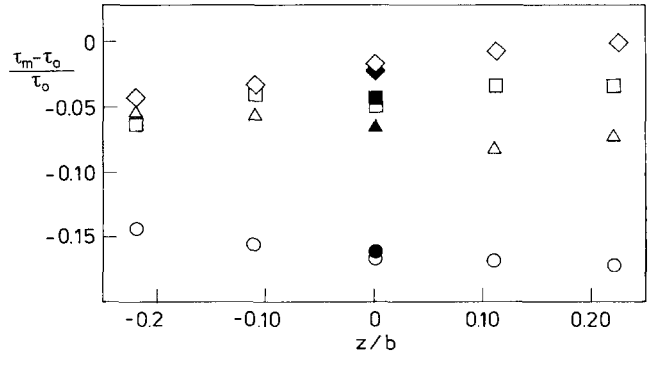

Fig. 8. Spanwise distribution of local skin friction reduction, measured with Preston tube. Data given for various downstream locations $\xi = (x - x_o)/\delta_o$. Solid symbols indicate span averaged value. ○ ≙ $\xi = 31$, △ ≙ $\xi = 63$, □ ≙ $\xi = 95$, ◇ ≙ $\xi = 127$

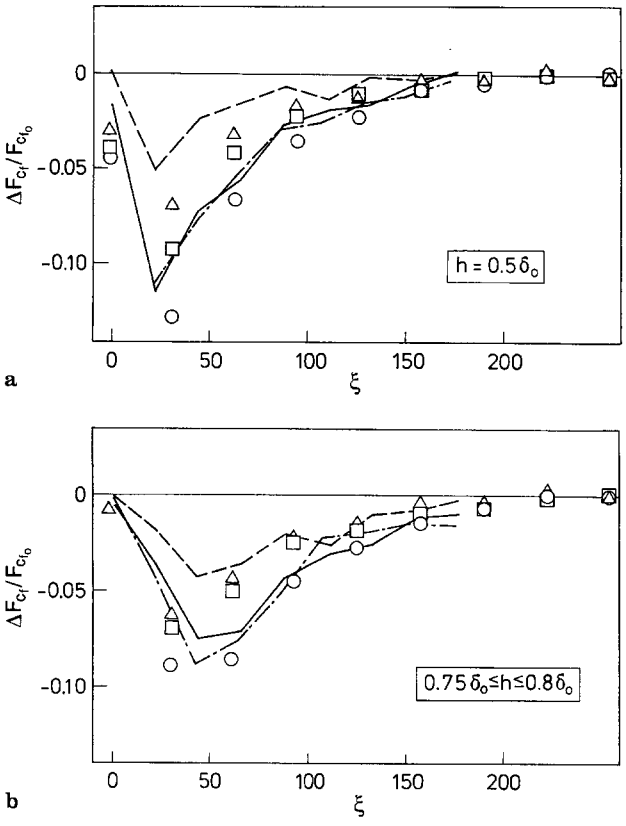

Fig. 9a, b. Skin friction drag savings ΔF_{cf} as a fraction of unmanipulated skin friction drag F_{cfo}, versus normalized distance ξ downstream. The drag force F is measured with the drag balance shown in Fig. 4. Ribbon manipulator: △ ≙ single, $c=1.276\delta_o=30$ mm. □ ≙ single, $c=2.552\delta_o=60$ mm. ○ ≙ tandem, $c=1.276\delta_o=30$ mm, $s=11.5\delta_o$. $U=15.6$ m/s, $Re_\theta=2{,}930$.

Airfoil (NACA 0009) manipulator: tandem, $c=1.15\delta_o=40$ mm;
-·- $\alpha=0$, $U=22.4$ m/s, $Re_\theta=5{,}760$, $Re_c=52{,}000$, $s=7.78\delta_o$;
—— $\alpha=0$, $U=37.9$ m/s, $Re_\theta=8{,}850$, $Re_c=96{,}000$, $s=8.0\delta_o$;
Wire manipulator: tandem, $d=0.5+0.2$ mm diameter; $c=0.5$ mm;
--- $U=37.9$ m/s, $Re_\theta=8{,}850$, $Re_c=1{,}200$, $s=8.0\delta_o$.

a All devices: height: $h=0.5\delta_o$;
b Ribbon manipulator: $h=0.75\delta_o$;
(Airfoil (NACA 0009) manipulator:
-·- $h=0.77\delta_o$,
—— $h=0.8\delta_o$;
Wire manipulator:
---- $h=0.8\delta_o$)

LEBUs used here lie within 1% of the empirical curve of A.F. Messiter (see Schlichting 1982), indicating that the device drag is due primarily to laminar skin friction drag. In this respect, ribbon-type LEBUs perform considerably better than the NACA 0009 profiles used at higher Reynolds numbers (Lynn et al. 1989; Anders and Watson 1985; Sahlin et al. 1988).

The accurate determination of net drag in an experimental set-up other than a towing tank, where the total drag is measured directly, is not a trivial matter. Assuming that the flow is suitably two-dimensional before a manipulator is introduced into the flow, there is no reason a priori to assume that the flow will remain so once a manipulator is introduced. This is possibly a source of error in previous point-wise measurements made along the center line. To illustrate this point, Preston tube measurements were made across the span at various streamwise locations with and without the tandem

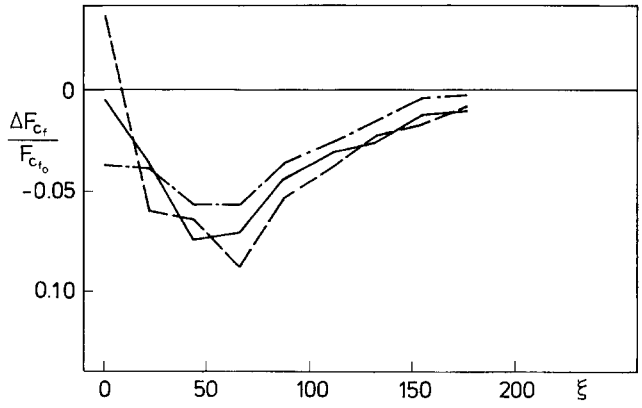

Fig. 10. The influence of the angle of attack on the skin friction reduction. The figure shows skin friction savings as a fraction of the unmanipulated skin friction drag, versus the normalized distance downstream of a NACA 0009 tandem LEBU. "High speed" case with $U=37.8$ m/s, $Re_\theta=8{,}850$, $Re_c=96{,}000$, $h=0.8\delta_o$, $s=8\delta_o$, $c=1.18\delta_o=40$ mm. --- $\alpha=-2°$, —— $\alpha=0°$, -·- $\alpha=+2°$

30 mm chord ribbon manipulator at $h=0.5\delta_o$. The results, presented in Fig. 8, show that not only is the magnitude of reduction not uniform across the span, but this non-uniformity varies with downstream distance. In our flow, the span-averaged mean agrees well with the centerline point (as well as with the drag balance measurement) for each location. This will not, however, necessarily be the case in all flows, and when determining total drag reduction by local measurements, any error will be reflected in the calculation of the total drag. It should be pointed out here that since direct measurements indicate that the net change in total drag is a less than 1% increase, any measurement technique must be accurate to better than 1%. Due to the inherent difficulties of Preston tube measurements in manipulated flows as well as the above mentioned problems of three-dimensionality, we do not rely on them in any way for determining net drag; we have made these measurements only to illustrate one possible source of error when making net drag determinations using pointwise measurements.

Our experiments rely on our floating element balance. With this device, the shear force F_{cf} is determined on the test plate in 9 different locations under and downstream of the LEBU. Without the LEBU, the undisturbed boundary layer produces a higher shear force F_{cfo} in the same 9 locations. The difference $\Delta F_{cf}=(F_{cf}-F_{cfo})$ represents the skin friction savings and is normalized in our plots with the undisturbed value F_{cfo}.

The skin friction distributions obtained for the LEBU devices shown in Fig. 9a and b indicate that by the end of the test plate the local skin friction has returned to within 1% of its unmanipulated value in all cases, indicating that the recovery length for the skin friction distribution downstream of LEBU manipulators is on the order of $200\delta_o$. The skin friction distributions also show that the WIRE device produces a smaller reduction in local skin friction relative to the LEBU device, with the maximum reduction occurring at approximately the same location downstream of the device. There appears to be little variation between the two "high speed" cases. The skin friction distribution measured for the $h=0.75\delta_o$ tandem ribbon device agrees well with the other published direct

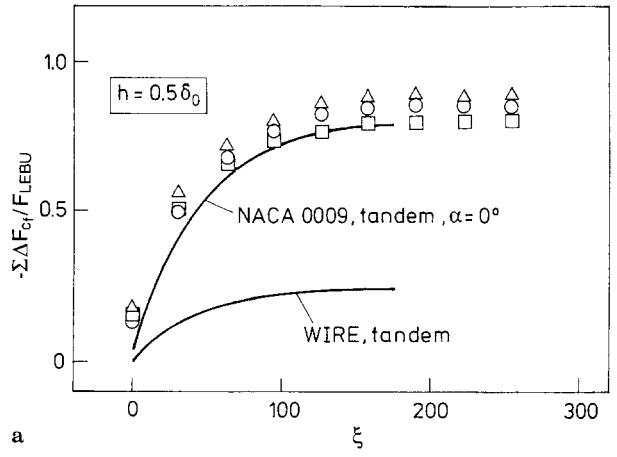

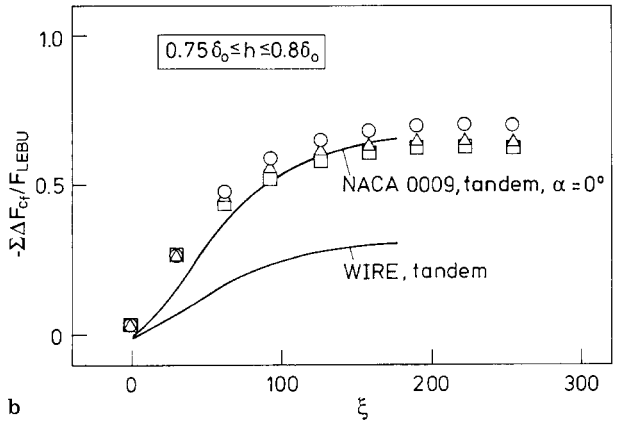

Fig. 11a, b. Recovery of the device drag. Cumulative skin friction savings as a fraction of device drag, versus downstream distance. Manipulator height (**a**) $h=0.5\delta_o$, (**b**) $0.75\delta_o \leqslant h \leqslant 0.80\delta_o$. Symbols for the ribbon manipulators as in Fig. 9: △ ≙ single blade 30 mm; □ ≙ single blade 60 mm; ○ ≙ tandem, 2 blades with 30 mm chord

measurements of skin friction distributions for ribbon LEBUs, plotted in Fig. 2. The maximum skin friction reduction was obtained in the tandem $0.5\delta_o$ case, and is on the order of 12–13% (averaged over $30\delta_o$). (Correcting for this averaging effect indicates that the maximum local reduction is approximately 15–16%).

The relaxation distances and the maximum skin friction reductions for the LEBU devices with angles of attack of $+2°$ and $-2°$ are rather similar to the $0°$ case; see Fig. 10. However, the upstream effects are very different. The $+2°$ case shows an upstream decrease in skin friction, whereas the $-2°$ case shows an upstream increase in skin friction. This effect has also been measured using sublayer fences for ribbon type LEBUs at angles of attack (Lynn 1987).

The integral of the skin friction drag savings as a fraction of the device drag is shown in Fig. 11a and b, indicating that in spite of its relatively small skin friction reduction, the most efficient LEBU configuration is the 30 mm chord single LEBU at $h=0.5\delta_o$. This configuration, which has the lowest device drag, results in approximately 90% of the device drag being recovered in skin friction savings. This result is contrary to the widely-held belief that a "tandem" configuration performs best.[5] The

[5] The same observation has been made by Sahlin et al. (1988).

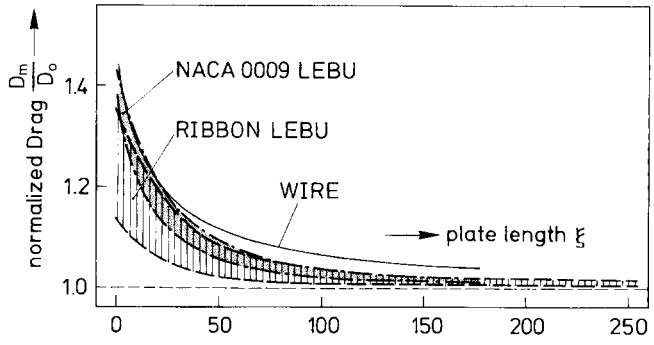

Fig. 12. Ratio of total drag D_m with a device to total drag without a device D_o versus downstream distance ξ for NACA 0009 LEBU's, ribbon-type LEBU's and WIRE devices

NACA 0009 results indicate that due to their larger device drag (30% above laminar skin friction value), their best performance was a recovery of 75–80% of their device drag. Comparison with the WIRE devices shows that a merely wake-producing device recovers only about 25–30% of its device drag.[6] The next-to-last row in Tables 2a, b, and c (F_{LEBU}/F_o) shows the total drag force on the manipulator (F_{LEBU}) as a fraction of the total measured skin friction drag on the unmanipulated flat plate (F_o). The device drag ranges from approximately 6.6% of the skin friction drag in the worst case (large angle of attack and thick device) to as little as 2.2% for the single ribbon device. At non-zero angles of attack the LEBU performance was in all cases poorer than in the zero angle of attack cases, with the difference becoming more pronounced at the highest speed. This is entirely due to the device drag increase; the integrated skin friction reductions are identical.

The fact that the single ribbon type LEBU is the most efficient configuration is reflected also in the ratios of the total drag on the LEBU system to the drag on just the flat plate, see Fig. 12. The resulting best performance, obtained for the 30 mm single LEBU $h=0.5\delta_o$ configuration, is a net increase of 0.25% in total drag. The WIRE device produced a consistent net increase of 4% in all configurations. These plots show clearly which type of LEBU most efficiently recovers its own device drag and reveal that varying the distribution of the device chord (i.e., 60 mm "single" versus 30 mm "tandem") affects the drag recovery distribution very little. In the last row of Tables 2a, b, and c, the final realized performance for each manipulator is presented as the ratio of the total drag on the manipulator plus flat plate system (F_m) to the total skin friction drag on the unmanipulated flat plate (F_o).

When the integrated skin friction reduction is plotted against the device drag[7] for all cases tested here, some sense can be made of the variation in LEBU performance between the different configurations. Figure 13 reveals that, within a "family" (determined by device height), the skin friction reduction is proportional to the device drag. The ribbon data,

[6] The aspect of "blade" versus "wake" effect of the blade and wire LEBU's is discussed in some detail in the work of Narasimha and Sreenivasan (1988).

[7] The idea that the skin friction reduction varies with device drag was first suggested by Sahlin et al. (1988).

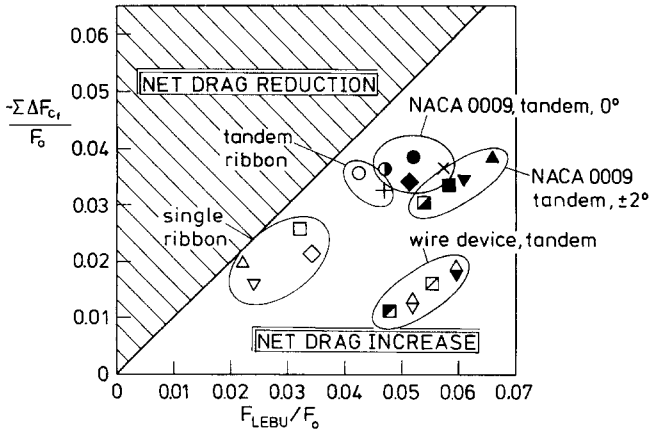

Fig. 13. Skin friction savings $\sum \Delta F_{cf}$ as a fraction of unmanipulated skin friction drag F_o versus the ratio of device drag F_{LEBU} to unmanipulated skin friction drag F_o. Tandem spacing $s=8\delta_o$.
Ribbon tandem LEBU's $\alpha=0°$:
$c=1.276\delta_o$, $Re_c \approx 30{,}000$: $\bigcirc \triangleq h=0.5\delta_o$, $+\triangleq h=0.75\delta_o$.
Ribbon single LEBU's $\alpha=0°$:
$c=1.276\delta_o$, $Re_c \approx 30{,}000$: $\triangle \triangleq h=0.5\delta_o$, $\triangledown \triangleq h=0.75\delta_o$;
$c=2.552\delta_o$, $Re_c \approx 60{,}000$: $\square \triangleq h=0.5\delta_o$, $\diamond \triangleq h=0.75\delta_o$

NACA 0009 tandem LEBU's:
$c=1.15\delta_o$,
$h=0.49\delta_o$; $Re_c=52{,}000$: $\bullet \triangleq \alpha=0°$
$h=0.77\delta_o$; $Re_c=57{,}000$: $\blacksquare \triangleq \alpha=+2°$; $\times \triangleq \alpha=0°$; $\blacktriangle \triangleq \alpha=-2°$

$c=1.18\delta_o$,
$h=0.50\delta_o$; $Re_c=88{,}000$: $\boxplus \triangleq \alpha=0°$
$h=0.80\delta_o$; $Re_c=96{,}000$: $\boxplus \triangleq \alpha=+2°$; $\blacklozenge \triangleq \alpha=0°$; $\blacktriangledown \triangleq \alpha=-2°$

Wire tandem devices:
$c=0.0144\delta_o$, $Re_c \approx 700$: $\boxplus \triangleq h=0.49\delta_o$, $\boxplus \triangleq h=0.77\delta_o$
$c=0.0148\delta_o$, $Re_c \approx 1200$: $\diamondsuit \triangleq h=0.50\delta_o$, $\diamondsuit \triangleq h=0.80\delta_o$

for example, then separates into two groups: The LEBUs at $h=0.5\delta_o$ lie on a line closer to the zero-net-change line (45° line) than do those at $h=0.75\delta_o$, indicating better performance at $h=0.5\delta_o$, independent of LEBU configuration. Within each family, increasing the duration of the manipulation (i.e., the length of the device), either by increasing device chord length or increasing the number of devices, results only in additional skin friction savings equal to and thus offset by the additional device drag. Changing the device height shifts the entire curve relative to the 45° line, although it did not shift the curve into the net drag reduction region above the 45° line.

The data from the NACA 0009 LEBUs show again that within a height family, the skin friction reduction is directly proportional to the device drag. As expected, the NACA 0009 profile LEBU data is displaced to the right (worse net drag performance), due to the higher device drag (the NACA 0009 profiles used had a C_D above the laminar skin friction value). The trend is the same; the $h=0.5\delta_o$ configuration is again better and angles of attack other than zero result in a shift further to the right.

The data for WIRE devices, also shown in Fig. 13, plot even further to the right. This poor performance is independent of the device height, indicating that the relatively small contribution of the wake to skin friction drag reduction is most likely a function of the momentum defect and is not due to coherent-structure-wake interactions. If only local measurements of skin friction are made, the performance of WIRE devices appears to improve as the device height decreases, due to the larger local skin friction reduction. The integrated skin friction reduction, however, remains proportional to the device drag.

The finding that LEBUs do not produce net drag reduction could be furnished only by precise measurements: There is in fact no theory available to reject this idea a priori. For example, if one considers a flow with a strong and well correlated fluctuation of its flow angle, it is conceivable that an airfoil may be able to reduce drag. This would require that the device drag be, at least partly, eliminated by the Katzmayr effect (Katzmayr 1922). Because it cannot be assumed that this particular effect is well known, a short explanation is given here: the Katzmayr effect can reduce or eliminate the drag of an airfoil if it is exposed to a flow of varying angle of attack. The maximum angle should not be small but should also not exceed the angle at which the flow on the airfoil separates. Under these circumstances the force vector of the airfoil can move into the forward quadrant, i.e., the airfoil can even generate thrust instead of drag. For this effect to be realized, the fluctuations must be well correlated over several chord lengths in the spanwise direction. However, as it turns out, the turbulence levels and the coherence of the angular fluctuations in a turbulent boundary layer are not sufficient for this effect to occur.

4 Conclusion

We have shown that ribbon type LEBUs perform better than NACA 0009 profile LEBUs, due to the ribbon LEBU's lower device drag. Both types of devices are far superior to wire type devices, which merely produce drag. Wire devices recover only about 25–30% of their device drag; NACA 0009 devices recover almost 80% of their device drag; and ribbon devices recover as much as 90% of their device drag. The difference in performance between wire type devices and devices with a chord length on the order of δ_o is most likely due to the effective destruction of large scale turbulent structures by the latter devices. The LEBU manipulators effectively prevent energetic turbulent events from reaching the outer boundary layer interface over a length on the order of a few device chord lengths, thus interrupting the turbulence production cycle (Mumford and Savill 1984). The reduction in skin friction due to this decoupling has been shown here to be roughly proportional to the device chord and hence to the device drag (i.e., there is no added benefit to repeated manipulation or increasing the chord length of the device beyond $c=\delta_o$). This result disproves the belief that a tandem configuration is the optimum configuration for LEBU manipulators. The better performance of ribbon devices as compared to NACA 0009 devices appears to be due simply to their lower device drag. This improvement, however, merely reduces the amount of net drag increase. Even the most efficient ribbon type LEBU configuration resulted in a 0.25% net increase in total drag. The possibility of successfully achieving a net drag reduction is small. All reasonable extrapolations of the data in Fig. 13 appear to intersect the break-even line at the origin, indicating that while performance can be improved up to a point by reducing device drag, further

reducing the device drag simply reduces the net drag increase proportionally. It looks as if the best that can be achieved is a zero drag increase.

References

Anders JB (1986) Large eddy breakup devices as low Reynolds number airfoils. NASA SAE Technical Paper 861769

Anders JB (1989) LEBU drag reduction in high Reynolds number boundary layers. AIAA-Paper 89-1011

Anders JB; Watson RD (1985) Airfoil large-eddy breakup devices for turbulent drag reduction. AIAA-Paper 85-0520

Anders JB; Hefner JN; Bushnell DM (1984) Performance of large-eddy breakup devices at post-transitional Reynolds numbers. AIAA-Paper 84-0345

Bandyopadhyay PR (1985) The performance of smooth-wall drag reducing outer-layer devices in rough-wall boundary layers. AIAA-Paper 85-0558

Bandyopadhyay PR (1986) Mean flow in turbulent boundary layers disturbed to alter skin friction. J Fluids Eng 108: 127–40

Bechert DW; Hoppe G; Reif W-E (1985) On the drag reduction of the shark skin. AIAA-Paper 85-0546

Bertelrud A; Truong TV; Avellan F (1982) Drag reduction in turbulent boundary layers using ribbons. AIAA-Paper 82-1370

Blackwelder RF; Chang SI (1986) Length scales and correlations in a LEBU modified turbulent boundary layer. AIAA-Paper 86-0287

Bonnet JP; Delville J; Lemay J (1987) Study of LEBU's modified turbulent boundary layer by use of passive temperature contamination. International Conference on Turbulent Drag Reduction by Passive Means, The Royal Aeronautical Society, London, Sept. 1987

Bruns J; Dengel P; Fernholz HH (1992) Mean flow and turbulence measurements in an incompressible two-dimensional turbulent boundary layer. Institutsbericht 02/92, Hermann-Föttinger-Institut, TU Berlin

Corke TC (1981) A new view on origin, role and manipulation of large scales in turbulent boundary layers. Ph.D. Thesis, Illinois Institute of Technology, Chicago, Illinois, December 1981

Corke TC; Guezennec YG; Nagib HM (1979) Modification in drag of turbulent boundary layers resulting from manipulation of large-scale structures. Presented at the AIAA Symposium on Viscous Drag Reduction, Dallas, Texas, Nov. 7–8, 1979

Corke TC; Nagib HM; Guezennec YG (1982) A new view on origin, role and manipulation of large scales in turbulent boundary layers. NASA CR 165861

Coustols E; Cousteix J (1985) Reduction du frottement turbulent: moderateurs de turbulence. 22ème Colloque d'Aerodynamique Appliquée, Lille, France, Nov. 13–15, 1985

Guezennec YG; Nagib HM (1990) Documentation of mechanisms leading to net drag reduction in manipulated turbulent boundary layers. AIAA J 28: 245–252

Head MR; Rechenberg I (1962) The Preston tube as a means of measuring skin friction. J Fluid Mech 14: 1–17

Hefner JN; Weinstein LM; Bushnell DM (1981) Large-eddy breakup scheme for turbulent viscous drag reduction. AIAA-Paper 81-26507

Hefner JN; Anders JB; Bushnell DM (1983) Alteration of outer flow structures for turbulent drag reduction. AIAA-Paper 83-0293

Katzmayr R (1922) Über das Verhalten von Flügelflächen bei periodischen Änderungen der Geschwindigkeitsrichtung. Zeitschrift für Flugtechnik und Motorluftschiffahrt, 6. Heft, 13, Jahrg., 80–82. And: 7. Heft, 13, Jahrg., 95–101

Lemay J; Provençal D; Gourdeau R; Nguyen VD; Dickinson J (1985) More detailed measurements behind turbulence manipulators including tandem devices using servo-controlled balances. AIAA-Paper 85-0521

Lemay J; Savill AM; Bonnet JP; Delville J (1989) Some similarities between turbulent boundary layers manipulated by thin and thick flat plate manipulators. Turbulent Shear Flows 6, Springer-Verlag, Berlin

Lynn TB (1987) Manipulation of the structure of a turbulent boundary layer. Ph.D. Thesis, Yale University, New Haven, CT., May

Lynn TB (1989) Structures in a turbulent boundary layer. Adv Turb 2: 449–454, Springer-Verlag, Berlin

Lynn TB; Gerich DA; Bechert DW (1989) LEBU-manipulated flat plate boundary layers: skin-friction and device drag measured directly. IAHR Drag Reduction '89 Conference, Davos, Switzerland, July

Mangus JF (1984) Measurement of drag and bursting frequency downstream of tandem spanwise ribbons in a turbulent boundary layer. Master's Thesis, Massachusetts Institute of Technology, Cambridge, MA, USA

Miley SJ (1982) A catalog of low Reynolds number airfoil data for wind turbine applications. Dept. of Aerospace Engineering, Texas A&M University, College Station, Texas 77843, USA, Report RFP-3387, UC60 and: Addendum (1985)

Morse PM; Ingard KU (1968) 1968 Theoretical acoustics. New York: McGraw-Hill

Mumford JC; Savill AM (1984) Parametric studies of flat plate turbulence manipulators including direct drag results and Laser flow visualization. ASME Symposium on Turbulent and Laminar Boundary Layers, New Orleans, Louisiana

Nagib HM; Guezennec YG; Plesniak M (1984) Progress report for NASA Langley Research Grant, NSG-1591

Narasimha R; Sreenivasan KR (1988) Flat plate drag reduction by turbulence manipulation. Sadhana, India, Vol. 12, Parts 1 & 2, February, 5–30

Nguyen VD; Dickinson J; Chalifour Y; Anderson J; Lemay J; Haeberle D; Larose G (1984) Some experimental observations of the law of the wall behind Large-Eddy Breakup Devices using servo-controlled skin friction balances. AIAA-Paper 84-0346

Nguyen VD; Savill AM; Westphal RV (1987) Skin friction measurements following manipulation of a turbulent boundary layer. AIAA J 25: 498–500

Papathanasiou AG; Nagel RT (1986) Boundary layer control by acoustic excitation. AIAA-Paper 86-1954

Plesniak MW (1984) Optimized manipulation of turbulent boundary layers aimed at net drag reduction. Master's Thesis, Illinois Institute of Technology, Chicago, Illinois, USA

Poddar K; Van Atta CW (1985) Turbulent boundary layer drag reduction on an axisymetric body. 5th Symposium on Turbulent Shear Flows, Cornell University, Aug. 7–9, 1985

Poll DIA; Westland PG (1987) A study of LEBU performance by direct total force measurements. Symposium on Turbulent Drag Reduction by Passive Means, The Royal Aeronautical Society, London, Sept. 1987

Pollard A; Savill AM; Thomann HH (1989) Turbulent pipe flow manipulation and modelling. In: Drag Reduction in Fluid Flows: Techniques for Friction Control, 27–34, Eds. Sellin RHJ; Moses RT, Ellis Horwood, Chichester

Prabhu A; Vasudevan B; Kailasnath P; Kulkarmi RS; Narasimha R (1987) Blade manipulators in channel flow. Proceedings IUTAM Symposium on Turbulence Management and Relaminarisation, Bangalore, 97–108, Springer-Verlag, Berlin/New York

Rashidnia N; Falco RE (1986) Changes in the turbulent boundary layer structure associated with net drag reduction by outer layer manipulators. Michigan State University, Turbulent Structures Lab Report TSL-86-1, May 1986

Sahlin A; Alfredsson PH; Johansson AV (1986) Direct drag measurements for a flat plate with passive boundary layer manipulators. Phys Fluids 29: 696–700

Sahlin A; Johansson AV; Alfredsson PH (1988) The possibility of drag reduction by outer layer manipulators in turbulent boundary layers. Phys Fluids 31: 2814–20

Savill AM (1987) On the manner in which outer layer disturbances affect turbulent boundary layer skin friction. Advances in Turbulence, G. Comte-Bellot and J. Mathieu, eds., Springer-Verlag, Berlin

Schlichting H (1982) Grenzschicht-Theorie, Karlsruhe: Verlag G. Braun

Veuve M; Truong TV; Ryhming IL (1989) Detailed measurements downstream of a tandem manipulator in pressure gradients. Presented at the Symposium on Drag Reduction, Lausanne, Switzerland, July 1989

Westphal RV (1986) Skin friction and Reynolds stress measurements for a turbulent boundary layer following manipulation using flat plates. AIAA-Paper 86-0283